

# An integrated fluorescence detection system for lab-on-a-chip applications†‡

Lukas Novak, Pavel Neuzil,\* Juergen Pipper, Yi Zhang and Shinhan Lee

Received 17th August 2006, Accepted 2nd November 2006

First published as an Advance Article on the web 21st November 2006

DOI: 10.1039/b611745g

We present a low-cost miniaturized fluorescence detection system for lab-on-a-chip applications with a sensitivity in the low nanomolar range; a built-in lock-in amplifier enables measurements under ambient light.

The main purpose of a lab-on-a-chip (LOC) is to simplify and automate labor intensive, time consuming and costly laboratory procedures for applications, such as drug discovery, pathogen identification or (bio)chemical sensing.<sup>1</sup> A typical LOC consists of a number of components like sample inlets, reaction chambers, mixers, detectors, *etc.* Due to their robustness, high signal-to-noise ratio, and sensitivity the optical detection methods still dominate over others. However, with a few exceptions,<sup>2</sup> the optical detection is commonly accomplished using a microscope located off-chip.<sup>3</sup>

Optical systems for the detection of fluorescent signals typically consist<sup>4</sup> of the following components: a light source for emitting light at a suitable wavelength range, excitation filter to eliminate unwanted light, dichroic mirror for the optical separation of excitation and emission channels, emission filter, and a detector with electronics for signal processing. Mercury lamps and lasers have been traditionally used as light sources. As they are both bulky and expensive, their combination with LOC devices results in a “chip-in-a-lab” rather than a LOC.

In the last few years, fluorescence systems based on light emitting diodes (LED) became popular<sup>5</sup> for their low cost. LEDs are more than a thousand times cheaper than alternative light sources and they are also superior to lasers due to their long lifetime. On the top of that, the LED's light output as well as semiconductor lasers<sup>7</sup> can be modulated. As the LEDs are only a few mm in diameter as well as in length, they can be integrated into portable LOC systems, such as a real-time PCR system.<sup>6</sup> An elegant solution was demonstrated,<sup>7</sup> in which four channels were implemented in a semi-simultaneous fashion. However, the system might be still too bulky for LOC applications as its size is much bigger than that of a typical LOC device.

The amplitude of the excitation light has to be kept low to avoid bleaching effects, thus producing fluorescence light with a low intensity. Therefore, a high gain amplification of the fluorescence signal is required. The most popular detectors found in fluorescence detection systems are photo multiplier tubes (PMTs), avalanche photodiodes, and photon counting modules (PCMs).

Such systems are complex, bulky, and costly, and usually require operation in (complete) darkness.

We have decided to develop a fluorescence detection system, which is simple, miniaturized and cost effective. Currently, there are mass produced cheap optical systems occupying a total volume of about 1 cm<sup>3</sup> or less. A typical example is a pickup head of a digital versatile disc (DVD). The head consists of a light source (typically a red laser diode), first filter (or no filter), beam splitter, mirror to reflect light perpendicularly to the laser location, focusing optics, actuator, and a photodiode as detector. Our design was inspired by the DVD pickup head with a few modifications. It consisted of a blue LED with collimating optics, excitation and detection filters, dichroic mirror and photodiode as the light detector (see Fig. 1).

The optical path of the system can be split into two parts: excitation and detection. The excitation path starts with a light source. We have chosen a turquoise colored LED model ETG-5CE490-15 (ETG. Corp.). The LED has a peak emission wavelength of 490 nm with a luminous intensity of 6 cd (candela), and a viewing angle of 15°. Due to lacking collimation, we experienced power losses over the length of the optical path. Therefore, the light had to be collimated. This was done by milling the top of the LED plastic cover down to a distance of 0.5 mm from the LED chip. The cut surface was then flattened by aluminium oxide abrasive waterproof paper and polished by a conventional diamond paste.

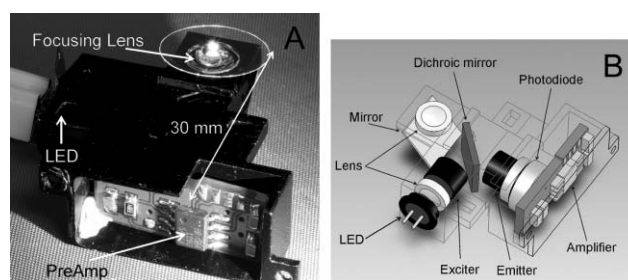


**Fig. 1** (A) A photograph of the integrated detection system, assembled in a metal housing. The location of the LED light source, focusing lens, and preamplifier are indicated by arrows. (B) Schematic of the optical system. Light emitted from the blue LED is collimated by a lens, passes through the excitation filter, and is reflected from the dichroic mirror; after being redirected by a conventional mirror, it is focused on a sample by a second collimating lens. The fluorescence light from the sample is then collimated by the same lens, redirected by the mirror, passes through the dichroic mirror, and is detected by a photodiode after being filtered by an emitter filter. The signal from the photodiode is immediately amplified by the first amplification stage, which is also located inside the housing.

*Institute of Bioengineering and Nanotechnology, 31 Biopolis Way, The Nanos, #04-01, Singapore 138669*

† The HTML version of this article has been enhanced with colour images.

‡ Electronic supplementary information (ESI) available: Measured and calculated optical properties of the fluorescent system. See DOI: 10.1039/b611745g

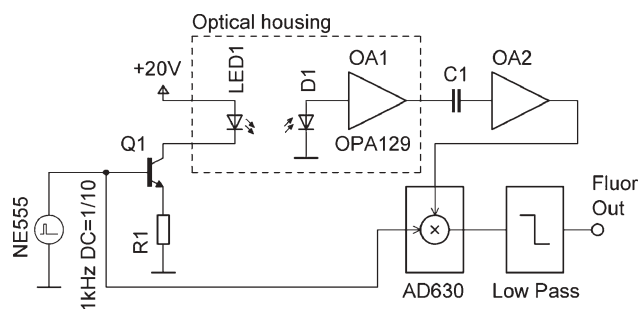


**Fig. 2** Simplified schematic of the electronic circuit for optical excitation and detection. The LED is powered by current pulses, generated by a pulse voltage generator NE555, and converted into current by transistor Q1. The fluorescence light, detected by a photodiode D1, is converted into a voltage by OA1. Its output voltage is then amplified by OA2, filtered by a demodulator AD630, followed by a low pass filter.

We selected Geltech<sup>TM</sup> molded glass aspheric lenses (Thorlabs, Inc.) for both light collimating and focusing on the sample. The lenses have a diameter of 6.35 mm, focal length of 3.1 mm, and numerical aperture (N.A.) of 0.68. Collimated light was then filtered by an exciter (ET470/40x, Chroma, Inc.), reflected two times by the dichroic (T495LP, Chroma, Inc.) and a conventional mirror (that was made by evaporation of aluminium onto silicon), and focused on the sample of interest by a second lens, thereby forming a circular shape of excitation light with a diameter of 480  $\mu\text{m}$ .

The detection path started with the collection of fluorescence light by the second lens. The fluorescence light passed through the dichroic mirror, was filtered by an emitter (ET525/50 m), and collected by a silicon photodiode (BPW21, Siemens, Inc.). Its radiant sensitive area of 7.34  $\text{mm}^2$  with a quantum yield of 0.8 resulted in an optical sensitivity of 10  $\text{nA lx}^{-1}$  (nanoamperes per lux).

Due to the low amplitude of the incident fluorescence light, the corresponding current generated by the photodiode (photocurrent) was first processed by a low-noise amplifier that was placed next to the photodiode in order to minimize the distance between the devices, thus reducing parasitic noise.

All the devices had to be mechanically connected to each other to form a stable and compact system. A highly integrated approach with the total size of a few millimetres was demonstrated earlier.<sup>8</sup> We have chosen a rather conventional approach. The housing for all the optical components including the first amplifier was designed in a computer aided design (CAD) program (SolidWorks 2006, Solid Works Corp.). The size of the housing was (width  $\times$  length  $\times$  height) 30 mm  $\times$  30 mm  $\times$  11 mm (see Fig. 1A). The housing was then manufactured by a computer numerical control (CNC) vertical milling method from an aluminium alloy AA 6060 and electrochemically blackened to suppress unwanted internal reflections. The optical power attenuation of all components was measured in both the excitation and emission direction (see Table S1 in electronic supplementary information<sup>†</sup>).

The overall optical transmission of the fluorescence system was found to be 51% and 56% in the excitation and emission directions. Most of the components showed an efficiency of 90% or higher. The optical performance of the system could be further improved by forming filters (made by evaporation of multilayers) directly on the surface of the lenses. This technique, together with

mounting the lenses directly onto the LED and the photodiode, would reduce the number of optical interfaces. That would also make the design more compact, thus increasing the transmission along the optical path.

The amplitude of the generated current by the photodiode is low and a technique to improve the signal to noise ratio has to be implemented. A direct approach based on highly sensitive devices was described earlier.<sup>9</sup>

Another commonly used technique is based on the “lock-in” amplifier.<sup>10</sup> The light source (LED) is first modulated at a frequency  $f$ . The demodulator works as narrow band pass filter allowing only signals at frequency  $f$  to pass. Combining these two techniques results in a high signal to noise ratio and insensitivity to ambient light. A miniaturized lock-in amplifier to detect fluorescence was described earlier<sup>11</sup> and our approach was similar (see Fig. 2). The LED was powered by current pulses with a frequency of  $f \approx 1$  kHz, duty cycle of 10% and current amplitude of 100 mA. These pulses were generated by an integrated circuit NE555 (ST Microelectronics, Inc.), followed by a bipolar transistor to achieve the desired current. Generated light from the LED passed through the optical system described earlier in this paper and the emitted fluorescence light was detected by the photodiode.

The generated photocurrent was converted into a voltage ( $I/V$ ) by an ultra low bias current operational amplifier OPA129 (Burr Brown, Inc.). Its resistor of 3.3  $\text{M}\Omega$  in the feedback loop yielded a trans-impedance gain of  $3.3 \times 10^6 \text{ V A}^{-1}$ . The output voltage of the OPA129 operational amplifier was processed by a simple high pass filter. It was then amplified by a second amplifier OA2 with a gain of 100. The high pass filter eliminated the DC component of the signal, which is necessary for the proper functioning of the lock-in amplifier. Additionally, this filtering process also eliminated a possible saturation of the OA2 due to ambient light.

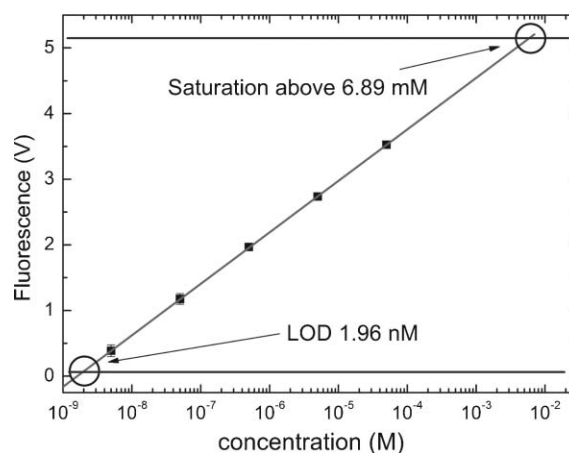


**Fig. 3** Detection limit using a dilution series of fluorescein in water conducted at 25 °C. Solid black squares are mean values of six individual measurements for the respective concentration; error bars represent the standard deviation; the solid line is a linear regression ( $r^2 = 0.999$ ) to the mean values; the solid horizontal line denotes the background of  $62.5 \pm 1.4$  mV. Three times signal-to-noise ratio (SNR 3) is 4.2 mV. The intersection of the linear regression with the background including SNR 3 indicates the LOD of the miniaturized fluorescence detection system, which is 1.96 nM (for the description of the experiment, see text). Saturation of the detector at 5.2 V determines the upper detection limit, which corresponds to a concentration of 6.89 mM.

The output of the OA2 was then processed by a demodulator AD630 (Analog Devices, Inc.), which used the pulses powering the LED as a reference. The demodulator output was filtered by a low pass filter of the 4th order. This configuration of lock-in amplifier worked as a filter with a bandwidth of 1.5 Hz around the frequency  $f$  of the LED reference signal. Due to the narrow band pass the system is insensitive to ambient light and other noise contributors.

To demonstrate the capability of the fluorescence detection system, we chose to run a set of experiments using a dilution series of fluorescein (see Fig. 3). It is one of the most popular fluorescent dyes used for biological and biochemical applications. As we have tested, the sample exhibited only negligible bleaching under the conditions of the experiment.

We placed a 1  $\mu$ L droplet containing different concentrations of fluorescein on top of a perfluorinated glass substrate, which was mounted in the focal plane of the miniaturized fluorescence detection system (see Fig. 1A). As reference, we used a control sample containing only de-ionized (DI) water. To estimate the probed volume, we experimented with droplets of different volumes ranging from 5  $\mu$ L down to 0.5  $\mu$ L. We found that the amplitude of the fluorescent signal was not affected by the droplet size. Therefore, we assumed that the probed volume was smaller than 0.5  $\mu$ L.

The dilution series started from a concentration of 50  $\mu$ M down to 5 nM. The amplitude of the fluorescence signal was plotted as a function of the concentration in logarithmic scale (see Fig. 3). The background noise of the detected system had a value of 62.5 mV. By extrapolation we found the limit of detection (LOD) of fluorescein to be 1.96 nM.

The sensitivity of our system could be increased by incorporation of an avalanche photodiode. However, this solution would be more costly and the electronics require a more complex design.

Established chip-based capillary electrophoresis systems based on laser induced fluorescence (LIF) typically reach 1 pM LOD.<sup>12</sup> The device described in this contribution has a LOD value 1000 times higher. Nevertheless, its sensitivity is sufficient to be used for real-time PCR applications as a typical commercial PCR system based on a PMT<sup>13</sup> has a sensitivity limit of around 5 nM.

The system described here is compact and low cost, making it a suitable candidate for an economical pocket real-time PCR system as well as other lab-on-a-chip applications, such as high resolution melting curve analysis, or hybridization experiments.

To demonstrate the system's applicability, we integrated the fluorescence detection unit with a PCR chip<sup>14</sup> creating a miniaturized real-time thermocycler (to be discussed elsewhere) and performed a melting curve analysis of the PCR products (see Fig. 4) in a 1  $\mu$ L volume. The sample was covered with 3  $\mu$ L of a mineral oil to prevent evaporation.

We are currently expanding the single channel system into three channels. The turquoise LED is replaced by a triple color LED, and the single bandpass filter set by a triple bandpass filter set. Each color of the LED is modulated at a unique frequency and has its own demodulator. This set-up allows the detection of up to three different wavelengths independently from each other. It will be used in real-time PCR applications allowing internal negative and positive controls (multiplexing).

We would like to thank Vitek Zahlava (Czech Technical University) for the PCB design and assembly. We are also grateful

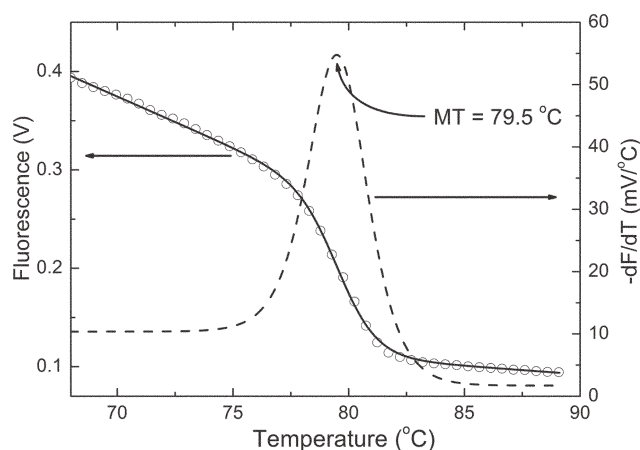


**Fig. 4** Melting curve analysis after performing a real-time PCR of the HA gene of the avian flu virus H5N1 using EvaGreen (Biotium, Inc.) as intercalator. A nonlinear fitting (solid line) of the raw data (open circles) based on a sigmoidal function was performed. Its negative derivative (dashed line) indicated a half melting temperature of 79.5 °C, which was close to that measured by a commercial thermocycler (79.8 °C by DNA Engine Opticon 2 from MJ Research, Inc.).

to the Institute of Bioengineering and Nanotechnology, Singapore, as well as the Agency for Science, Technology and Research, Singapore, for their financial support.

## Notes and references

- 1 R. Daw and J. Finkelstein, Lab on a chip, *Nature*, 2006, **442**, 367–418.
- 2 E. Verpoorte, Chip vision—optics for microchips, *Lab Chip*, 2003, **3**, 42N–52N.
- 3 G. M. Whitesides, The origin and future of microfluidics, *Nature*, 2006, **442**, 368–373.
- 4 M. E. Johnson and J. P. Landers, Fundamentals and practice for ultrasensitive laser-induced fluorescence detection in microanalytical systems, *Electrophoresis*, 2004, **25**, 3513–3527.
- 5 P. K. Dasgupta, I. Y. Eom, K. J. Morris and J. Z. Li, Light emitting diode-based detectors—Absorbance, fluorescence and spectroelectrochemical measurement in a planar flow-through cell, *Anal. Chim. Acta*, 2003, **500**, 337–364.
- 6 J. A. Higgins, S. Nasarabadi, J. S. Karns, D. R. Shelton, M. Cooper, A. Gbakima and R. P. Koopman, A handheld real time thermal cycler for bacterial pathogen detection, *Biosens. Bioelectron.*, 2003, **18**, 1115–1123.
- 7 P. Belgrader, S. Young, B. Yuan, M. Primeau, L. A. Christel, F. Pourahmadi and M. A. Northrup, A battery-powered notebook thermal cycler for rapid multiplex real-time PCR analysis, *Anal. Chem.*, 2001, **73**, 286–289.
- 8 A. E. Bruno, F. Maystre, B. Krattiger, P. Nussbaum and E. Gassmann, The pigtail approach to optical detection in capillary electrophoresis, *Trends Anal. Chem.*, 1994, **13**, 190–198.
- 9 L. Rovati and F. Docchio, Low-noise front end electronics for solid-state fluorimeters, *Rev. Sci. Instrum.*, 1999, **70**, 3759–3764.
- 10 J. H. Scofield, A frequency domain description of a lock-in amplifier, *Am. J. Phys.*, 1994, **62**, 129–133.
- 11 P. C. Hauser, C. L. C. Liang and B. Muller, A solid state instrument for fluorescence chemical sensors using a blue light-emitting diode of high intensity, *Meas. Sci. Technol.*, 1995, **6**, 1081–1085.
- 12 D. J. Harrison, A. Manz, Z. Fan, H. Ludi and H. M. Widmer, Capillary electrophoresis and sample injection systems integrated on a planar glass chip, *Anal. Chem.*, 1992, **64**, 1926–1932.
- 13 <http://www.corbettlifescience.com/control.cfm?page=Rotor%2DGene%5F6000%5F6&langID=1>, manual for Rotor-Gene.
- 14 P. Neuzil, J. Pipper and H. T. Ming, Disposable real-time microPCR device: lab-on-a-chip for a low cost, *Mol. BioSyst.*, 2006, **2**, 292–298.